

Effect of the measurement errors on one-sided Synthetic-RZ control charts for monitoring the ratio of two normal variables

Kim Duc Tran^{*1,3}, Thi Hien Nguyen², and Kim Phuc Tran³

¹International Chair in DS & XAI, International Research Institute for Artificial Intelligence and Data Science, Dong A University, Danang, Vietnam

²Laboratoire AGM, UMR CNRS 8088, CY Cergy Paris Université, Cergy, France

³Univ. Lille, ENSAIT, ULR 2461 – GEMTEX – Génie et Matériaux Textiles, F-59000 Lille, France

June 5, 2026

Abstract

In numerous industrial production settings, keeping track of the ratio formed by two normally distributed random variables is a task of considerable practical interest. The present work examines how measurement errors influence the behaviour of a pair of one-sided Synthetic control charts designed to monitor such a ratio (referred to here as Synthetic-RZ charts), with the analysis covering both the zero-state and the steady-state average run length (*ARL*). To incorporate measurement error into the operation of these charts, we adopt a linear covariate error model. We describe, step by step, how the parameters of the underlying model evolve as the process moves from an in-control to an out-of-control state, and we deliberately avoid the restrictive premise that the observed shift magnitude is unrelated to the measurement errors. The run length characteristics of the charts are obtained by means of a Markov chain formulation. A series of numerical experiments makes clear that measurement error erodes the detection capability of the charts. A particularly useful outcome of the investigation is that collecting several measurements on each inspected unit does not constitute an efficient remedy for the adverse influence of measurement error on the performance of the Synthetic-RZ charts.

Keywords Synthetic control chart, ratio distribution, measurement error, one-sided chart, linear covariate error, Markov chain.

*Corresponding author. Email: ductk@donga.edu.vn

1 Introduction

Statistical Process Control (SPC) has long served as an effective methodology for overseeing manufacturing operations in industry. Within the SPC toolkit, control charts occupy a central position because of their ability to flag departures of a process from its intended behaviour. A large body of work has been devoted to constructing charts that respond more rapidly to process shifts; representative contributions include Tran²², Tran et al.³¹, Yeong et al.³³, and Nguyen and Tran¹⁷. The earliest and arguably most popular scheme is the Shewhart chart, proposed by Shewhart²⁰, whose appeal lies chiefly in how straightforward it is to apply. That said, when shifts are small or of moderate magnitude, the Shewhart chart reacts more sluggishly than memory-based alternatives such as the CUSUM chart Brook and Evans¹ and the EWMA chart Hunter¹². The Synthetic chart, introduced by Wu and Spedding³², was conceived to retain the simplicity of the Shewhart philosophy while improving sensitivity. It operates by coupling a Shewhart sub-chart with a conforming run length (*CRL*) sub-chart, and has been reported to compete favourably with rival schemes when detecting a range of process shifts.

In a variety of industrial production contexts, the quantity that genuinely matters is the ratio of two normally distributed variables, and several concrete instances of this have been documented. Tran et al.²⁷ described a case drawn from battery-recycling facilities in Italy, in which the ratio of the weight of “recyclable batteries” to that of the “total batch” must be tracked so as to gauge the associated economic loss. A second illustration, from the food sector, was given by Celano and Castagliola⁴, where the quantity of interest is the weight ratio of “pumpkin seeds” to “flaxseeds”. Further manufacturing situations of this kind are noted in Tran et al.^{26,25}. A range of charts has accordingly been put forward for monitoring such a ratio, among them Nguyen et al.¹⁵; Tran and Knoth²³; Tran et al.^{26,24,25}. A Synthetic chart for this purpose—the Synthetic-RZ chart—was developed by Celano and Castagliola³. Their proposal, however, is two-sided, and because the distribution of the ratio of two normal variables is skewed, the chart turns out to be *ARL*-biased: situations arise in which the out-of-control *ARL* exceeds the in-control one. As a remedy, Nguyen et al.¹⁸ advocated running two distinct one-sided Synthetic charts, one tuned to detect a downward move in the ratio and the other an upward move. Relative to the two-sided design of Celano and Castagliola³, this pair of one-sided charts removes the *ARL*-bias and detects ratio shifts more effectively.

With a view to making ratio charts more usable in practice, attention has recently turned to the question of measurement error. The topic itself has a substantial literature—see, for instance, Linna et al.¹⁴, Tran et al.²⁸, Tran et al.²⁹, Tran et al.²¹, Tran and Tran³⁰, Yeong et al.³³, Cheng and Wang⁶, and Nguyen et al.¹⁶—and these works collectively demonstrate that mea-

surement error exerts a pronounced influence both on the control limits and on chart performance. In the specific setting of ratio charts, Tran et al.²⁷ were the first to examine the impact of measurement error, doing so for a Shewhart-RZ chart. Their analysis, however, rested on a fairly restrictive premise, namely that the observed process shift is independent of the measurement error. One contribution of the present paper is to dispense with that premise so as to obtain a more realistic treatment. Furthermore, while the effect of measurement error has by now been studied for the Shewhart-RZ and the EWMA-RZ charts, the Synthetic-RZ charts—which tend to strike a useful compromise between simplicity and detection ability—have not yet been investigated in this respect. We therefore study how measurement error affects the two one-sided Synthetic-RZ charts of Nguyen et al.¹⁸, representing the error through a linear covariate error model and deriving in detail how the process parameters change in the presence of error, again without invoking independence between the shift magnitude and the measurement errors.

The remainder of the paper proceeds as follows. Section 2 recalls briefly the sampling distribution of the ratio of two normal variables. Section 3 sets out a linear covariate error model for the ratio and establishes how the model parameters move from the in-control to the out-of-control state. Section 4 addresses the design and operation of the one-sided Synthetic-RZ charts when measurement error is present, and Section 5 reports the effect of measurement error on their performance. A worked example illustrating the use of one such chart under measurement error is given in Section 6, and Section 7 offers some closing comments.

2 A short overview of the sample distribution of the ratio

Let $\mathbf{W} = (X, Y)^\top$ be a bivariate normal random vector with mean vector $\boldsymbol{\mu}_W$ and variance–covariance matrix $\boldsymbol{\Sigma}_W$ given by

$$\boldsymbol{\mu}_W = \begin{bmatrix} \mu_X \\ \mu_Y \end{bmatrix} \quad \text{and} \quad \boldsymbol{\Sigma}_W = \begin{bmatrix} \sigma_X^2 & \rho\sigma_X\sigma_Y \\ \rho\sigma_X\sigma_Y & \sigma_Y^2 \end{bmatrix}. \quad (1)$$

Here ρ denotes the correlation between X and Y , while σ_X and σ_Y are their respective standard deviations and μ_X , μ_Y their means. The two coefficients of variation and the ratio of the standard deviations are then $\gamma_X = \frac{\sigma_X}{\mu_X}$, $\gamma_Y = \frac{\sigma_Y}{\mu_Y}$ and $\omega = \frac{\sigma_X}{\sigma_Y}$, respectively.

The ratio of X to Y is written $Z = X/Y$. The distribution of Z has been the subject of several investigations—e.g. Geary¹⁰, Hayya et al.¹¹, Pham-Gia et al.¹⁹. Cedilnik et al.² derived a general closed-form expression for its probability density function (*p.d.f.*), and its cumulative distribution function (*c.d.f.*) along with the inverse *c.d.f.* can be evaluated numerically following

Celano et al.⁵. Since these exact routes are somewhat cumbersome to apply, approximations are usually preferred. As shown by Celano and Castagliola⁴, provided the coefficients of variation of X and Y are not too large, Z admits the accurate approximation

$$F_Z(z|\gamma_X, \gamma_Y, \omega, \rho) \simeq \Phi\left(\frac{A}{B}\right), \quad (2)$$

with $\Phi(\cdot)$ the *c.d.f* of the standard normal distribution, and where the quantities A and B depend on z , γ_X , γ_Y , ω and ρ through

$$\begin{aligned} A &= \frac{z}{\gamma_Y} - \frac{\omega}{\gamma_X}, \\ B &= \sqrt{\omega^2 - 2\rho\omega z + z^2}. \end{aligned}$$

For a stable process whose quality variables are normally distributed, the spread of the population ought to be much smaller than its mean, so assuming small γ_X and γ_Y —and hence adopting the approximate distribution—is justified. Differentiating the *c.d.f* in (2) gives the *p.d.f* of Z as

$$f_Z(z|\gamma_X, \gamma_Y, \omega, \rho) \simeq \left(\frac{1}{B\gamma_Y} - \frac{(z - \rho\omega)A}{B^3}\right) \times \phi\left(\frac{A}{B}\right), \quad (3)$$

with $\phi(\cdot)$ the standard normal density.

An approximation to the inverse distribution function (*i.d.f*) $F_Z^{-1}(p|\gamma_X, \gamma_Y, \omega, \rho)$ of Z can be obtained in the same spirit, namely

$$F_Z^{-1}(p|\gamma_X, \gamma_Y, \omega, \rho) \simeq \begin{cases} \frac{-C_2 - \sqrt{C_2^2 - 4C_1C_3}}{2C_1} & \text{if } p \in (0, 0.5], \\ \frac{-C_2 + \sqrt{C_2^2 - 4C_1C_3}}{2C_1} & \text{if } p \in [0.5, 1), \end{cases} \quad (4)$$

where the coefficients C_1 , C_2 and C_3 depend on p , γ_X , γ_Y , ω and ρ via

$$\begin{aligned} C_1 &= \frac{1}{\gamma_Y^2} - \Phi^{-1}(p)^2, \\ C_2 &= 2\omega \left(\rho\Phi^{-1}(p)^2 - \frac{1}{\gamma_X\gamma_Y} \right), \\ C_3 &= \omega^2 \left(\frac{1}{\gamma_X^2} - \Phi^{-1}(p)^2 \right), \end{aligned}$$

and $\Phi^{-1}(\cdot)$ is the *i.d.f* of the standard normal distribution.

3 Linear covariate error model for the sample of the ratio

This section develops a linear covariate error model for the sample ratio and gives a precise account of how the process parameters are altered once a shift occurs in the presence of measurement error.

Return to the bivariate normal vector $\mathbf{W} \sim N(\boldsymbol{\mu}_{\mathbf{W}}, \boldsymbol{\Sigma}_{\mathbf{W}})$ introduced in (1). Suppose $\{\mathbf{W}_{i,1}, \mathbf{W}_{i,2}, \dots, \mathbf{W}_{i,n}\}$ is a collection of n independent draws from it, where $\mathbf{W}_{i,j} = (X_{i,j}, Y_{i,j})^\top$ is the quality characteristic of the j -th unit, $j = 1, \dots, n$, inspected at time i , $i = 1, 2, \dots$

Owing to measurement error, the *true* characteristic $\mathbf{W}_{i,j}$ cannot be observed directly; what is available instead is a set of $m \geq 1$ repeated readings on unit j at time i , say $\{\mathbf{W}_{i,j,1}^*, \mathbf{W}_{i,j,2}^*, \dots, \mathbf{W}_{i,j,m}^*\}$. Following the linear covariate error model of Linna and Woodall¹³, each reading relates to the true value through

$$\mathbf{W}_{i,j,k}^* = \mathbf{A} + \mathbf{B}\mathbf{W}_{i,j} + \boldsymbol{\varepsilon}_{i,j,k}, \quad k = 1, \dots, m, \quad (5)$$

in which $\mathbf{A} = (a_X, a_Y)^\top$ is a (2×1) vector of constants, \mathbf{B} is a (2×2) matrix and $\boldsymbol{\varepsilon}_{i,j,k} \sim N(\mathbf{0}, \boldsymbol{\Sigma}_M)$ is a bivariate normal vector independent of $\mathbf{W}_{i,j}$. Denoting by σ_{MX} and σ_{MY} the standard deviations of the measurement error in X and Y and by $\rho_M \in (-1, +1)$ their correlation, the covariance matrix of $\boldsymbol{\varepsilon}$ reads

$$\boldsymbol{\Sigma}_M = \begin{pmatrix} \sigma_{MX}^2 & \rho_M \sigma_{MX} \sigma_{MY} \\ \rho_M \sigma_{MX} \sigma_{MY} & \sigma_{MY}^2 \end{pmatrix}. \quad (6)$$

As in Tran et al.²⁷, we take $\mathbf{B} = \mathbf{I}_{2 \times 2}$, the identity matrix, which amounts to assuming a constant accuracy-error vector \mathbf{A} across the measurement range.

Because $\mathbf{W}_{i,j}$ itself is hidden, its sample mean over the repeated readings,

$$\overline{\mathbf{W}}_{i,j}^* = \frac{1}{m} \sum_{k=1}^m \mathbf{W}_{i,j,k}^* = \mathbf{A} + \mathbf{B}\mathbf{W}_{i,j} + \frac{1}{m} \sum_{k=1}^m \boldsymbol{\varepsilon}_{i,j,k}, \quad (7)$$

is commonly used in its place. Writing $\overline{\mathbf{W}}_{i,j}^* = (\bar{X}_{i,j}^*, \bar{Y}_{i,j}^*)$, it follows from (7) that this average is again a bivariate normal vector, with mean vector

$$\boldsymbol{\mu}_{\mathbf{W}^*} = \mathbf{A} + \mathbf{B}\boldsymbol{\mu}_{\mathbf{W}} \quad (8)$$

and variance–covariance matrix

$$\boldsymbol{\Sigma}_{\mathbf{W}^*} = \mathbf{B}\boldsymbol{\Sigma}_{\mathbf{W}}\mathbf{B}^\top + \frac{1}{m}\boldsymbol{\Sigma}_M = \boldsymbol{\Sigma}_{\mathbf{W}} + \frac{1}{m}\boldsymbol{\Sigma}_M. \quad (9)$$

Building on these expressions, we now trace how the process parameters respond to a shift under measurement error.

While the process is in control, write the mean vector of the true characteristic $\mathbf{W}_{i,j} = (X_{i,j}, Y_{i,j})$ as $\boldsymbol{\mu}_{\mathbf{0},\mathbf{W}} = (\mu_{0,X}, \mu_{0,Y})^\top$ and the correlation between $X_{i,j}$ and $Y_{i,j}$ as $\rho = \rho_0$, so that the mean ratio equals $z_0 = \frac{\mu_{0,X}}{\mu_{0,Y}}$. Suppose that, when the process becomes disturbed, the ratio moves from z_0 to $z_1 = \tau z_0$ (with τ the shift size) and the correlation moves from ρ_0 to ρ_1 . The change in z_0 corresponds to a displacement of $\boldsymbol{\mu}_{\mathbf{W}}$ from $\boldsymbol{\mu}_{\mathbf{0},\mathbf{W}}$ to

$\boldsymbol{\mu}_{1,\mathbf{W}} = (\mu_{0,X} + \delta_X \sigma_X, \mu_{0,Y} + \delta_Y \sigma_Y)^\top$, where δ_X and δ_Y measure the size of the mean shifts in $X_{i,j}$ and $Y_{i,j}$ and the two standard deviations σ_X and σ_Y are assumed equal. The out-of-control mean ratio is therefore

$$z_1 = \frac{\mu_{0,X} + \delta_X \sigma_X}{\mu_{0,Y} + \delta_Y \sigma_Y} = \tau \times z_0 = \tau \times \frac{\mu_{0,X}}{\mu_{0,Y}},$$

from which the shift size satisfies

$$\tau = \frac{1 + \delta_X \gamma_X}{1 + \delta_Y \gamma_Y},$$

or equivalently

$$1 + \delta_X \gamma_X = \tau(1 + \delta_Y \gamma_Y). \quad (10)$$

Writing the mean vector and covariance matrix of $\bar{\mathbf{W}}_{i,j}^*$ as

$$\boldsymbol{\mu}_{\mathbf{W}^*} = \begin{pmatrix} \mu_{X^*} \\ \mu_{Y^*} \end{pmatrix} \text{ and } \boldsymbol{\Sigma}_{\mathbf{W}^*} = \begin{pmatrix} \sigma_{X^*}^2 & \rho^* \sigma_{X^*} \sigma_{Y^*} \\ \rho^* \sigma_{X^*} \sigma_{Y^*} & \sigma_{Y^*}^2 \end{pmatrix}, \quad (11)$$

equations (8) and (9) yield

$$\mu_{X^*} = a_X + \mu_X + \delta_X \sigma_X, \quad (12)$$

$$\mu_{Y^*} = a_Y + \mu_Y + \delta_Y \sigma_Y, \quad (13)$$

$$\sigma_{X^*}^2 = \sigma_X^2 + \frac{\sigma_{MX}^2}{m}, \quad (14)$$

$$\sigma_{Y^*}^2 = \sigma_Y^2 + \frac{\sigma_{MY}^2}{m}, \quad (15)$$

$$\rho^* = \frac{\rho \sigma_X \sigma_Y + \rho_M \frac{\sigma_{MX} \sigma_{MY}}{m}}{\sigma_{X^*} \sigma_{Y^*}}. \quad (16)$$

Hence the coefficients of variation $\gamma_{X^*} = \frac{\sigma_{X^*}}{\mu_{X^*}}$ and $\gamma_{Y^*} = \frac{\sigma_{Y^*}}{\mu_{Y^*}}$ of $\bar{X}_{i,j}^*$ and $\bar{Y}_{i,j}^*$ become

$$\gamma_{X^*} = \frac{\sqrt{\sigma_X^2 + \frac{\sigma_{MX}^2}{m}}}{a_X + \mu_{0,X} + \delta_X \sigma_X}, \quad (17)$$

$$\gamma_{Y^*} = \frac{\sqrt{\sigma_Y^2 + \frac{\sigma_{MY}^2}{m}}}{a_Y + \mu_{0,Y} + \delta_Y \sigma_Y}. \quad (18)$$

Dividing the numerator of (17) by σ_X and the denominator by $\mu_{0,X}$, and then substituting $\tau(1 + \delta_Y \gamma_Y)$ for $1 + \delta_X \gamma_X$ according to (10), recasts γ_{X^*} as

$$\gamma_{X^*} = \frac{\sqrt{1 + \frac{\eta_X^2}{m}}}{1 + \delta_X \gamma_X + \theta_X} \times \gamma_X = \frac{\sqrt{1 + \frac{\eta_X^2}{m}}}{\tau(1 + \delta_Y \gamma_Y) + \theta_X} \times \gamma_X, \quad (19)$$

where $\eta_X = \frac{\sigma_{MX}}{\sigma_X}$, $\theta_X = \frac{a_X}{\mu_{0,X}}$ and $\gamma_X = \frac{\sigma_X}{\mu_{0,X}}$.

In the same manner, γ_{Y^*} from (18) and ρ^* from (16) take the forms

$$\gamma_{Y^*} = \frac{\sqrt{1 + \frac{\eta_Y^2}{m}}}{1 + \delta_Y \gamma_Y + \theta_Y} \times \gamma_Y, \quad (20)$$

$$\rho^* = \frac{\rho + \rho_M \frac{\eta_X \eta_Y}{m}}{\sqrt{1 + \eta_X^2/m} \sqrt{1 + \eta_Y^2/m}}, \quad (21)$$

with $\eta_Y = \frac{\sigma_{MY}}{\sigma_Y}$, $\theta_Y = \frac{a_Y}{\mu_{0,Y}}$ and $\gamma_Y = \frac{\sigma_Y}{\mu_{0,Y}}$.

Likewise, the ratio of standard deviations $\omega^* = \frac{\sigma_{X^*}}{\sigma_{Y^*}}$ equals

$$\omega^* = \sqrt{\frac{1 + \frac{\eta_X^2}{m}}{1 + \frac{\eta_Y^2}{m}}} \times \omega, \quad (22)$$

where $\omega = \frac{\sigma_X}{\sigma_Y}$.

With this notation, the in-control and out-of-control ratios in the presence of measurement error are

$$z_0^* = \frac{\mu_{0,X^*}}{\mu_{0,Y^*}} = \frac{\mu_{0,X} + a_X}{\mu_{0,Y} + a_Y} = \frac{1 + \theta_X}{1 + \theta_Y} \times z_0, \quad (23)$$

$$z_1^* = \frac{\mu_{1,X^*}}{\mu_{1,Y^*}} = \frac{a_X + \mu_{0,X} + \delta_X \sigma_X}{a_Y + \mu_{0,Y} + \delta_Y \sigma_Y} = \frac{1 + \theta_X + \delta_X \gamma_X}{1 + \theta_Y + \delta_Y \gamma_Y} \times z_0. \quad (24)$$

Equations (23)–(24) make clear that, in general, $z_1^* \neq \tau z_0^*$. This is precisely where our treatment departs from Tran et al.²⁷, who assumed the observed shift size to be independent of the measurement error; abandoning that assumption affords a more realistic description of how measurement error bears on ratio control charts.

4 Design and implementation of the Synthetic-RZ control chart with measurement error

4.1 Distribution of the monitored statistic

When measurement error is present, the statistic being monitored takes the form

$$\hat{Z}_i^* = \frac{\hat{\mu}_{X_i^*}}{\hat{\mu}_{Y_i^*}} = \frac{\bar{X}_i^*}{\bar{Y}_i^*}, \quad (25)$$

with $\bar{X}_i^* = \frac{1}{n} \sum_{j=1}^n \bar{X}_{i,j}^*$ and $\bar{Y}_i^* = \frac{1}{n} \sum_{j=1}^n \bar{Y}_{i,j}^*$, where $\bar{X}_{i,j}^*$ and $\bar{Y}_{i,j}^*$ are the components of the vector $\bar{\mathbf{W}}_{i,j}^*$ of (7).

By construction, $\bar{X}_i^* \sim N(\mu_{X^*}, \frac{\sigma_{X^*}}{\sqrt{n}})$ and $\bar{Y}_i^* \sim N(\mu_{Y^*}, \frac{\sigma_{Y^*}}{\sqrt{n}})$, so the coefficients of variation of \bar{X}_i^* and \bar{Y}_i^* are

$$\gamma_{\bar{X}^*} = \frac{\sigma_{X^*}}{\mu_{X^*}\sqrt{n}} = \frac{\gamma_{X^*}}{\sqrt{n}}, \quad (26)$$

$$\gamma_{\bar{Y}^*} = \frac{\sigma_{Y^*}}{\mu_{Y^*}\sqrt{n}} = \frac{\gamma_{Y^*}}{\sqrt{n}}, \quad (27)$$

while the ratio of their standard deviations ω_i^* is

$$\omega_i^* = \frac{\sigma_{X^*}/\sqrt{n}}{\sigma_{Y^*}/\sqrt{n}} = \frac{\sigma_{X^*}}{\sigma_{Y^*}} = \omega^*. \quad (28)$$

The *c.d.f* and the *i.d.f* of \hat{Z}_i^* can accordingly be written as

$$F_{\hat{Z}_i^*}(z | n, \gamma_{X^*}, \gamma_{Y^*}, z_0^*, \rho_0^*) = F_{Z^*}\left(z | \frac{\gamma_{X^*}}{\sqrt{n}}, \frac{\gamma_{Y^*}}{\sqrt{n}}, \frac{z_0^*\gamma_{X^*}}{\gamma_{Y^*}}, \rho_0^*\right), \quad (29)$$

$$F_{\hat{Z}_i^*}^{-1}(p | n, \gamma_{X^*}, \gamma_{Y^*}, z_0^*, \rho_0^*) = F_{Z^*}^{-1}\left(p | \frac{\gamma_{X^*}}{\sqrt{n}}, \frac{\gamma_{Y^*}}{\sqrt{n}}, \frac{z_0^*\gamma_{X^*}}{\gamma_{Y^*}}, \rho_0^*\right), \quad (30)$$

where $F_{Z^*}(\dots)$ and $F_{Z^*}^{-1}(\dots)$ are those of (2) and (4), evaluated with the parameters γ_{X^*} , γ_{Y^*} , ω^* and ρ^* supplied by (19), (20), (22) and (21).

4.2 Design of the one-sided Synthetic-RZ control charts

A Synthetic chart pairs a Shewhart sub-chart with a conforming run length (*CRL*) sub-chart. The *CRL* counts the samples gathered between one non-conforming sample and the next; when no preceding nonconforming sample exists, it counts from the start of monitoring up to the first nonconforming sample Costa and Rahim⁷.

As noted in Section 1, the asymmetry of the distribution of Z (cf. (2)–(3)) means that a single two-sided Synthetic chart watching for both an increase and a decrease in Z is *ARL*-biased, as in Celano and Castagliola³. Following Nguyen et al.¹⁸, we sidestep this by employing two separate one-sided charts. The first is an upper-sided chart aimed at spotting an increase in the ratio (hereafter the ‘Synthetic-RZ⁺ chart’); the second is a lower-sided chart aimed at spotting a decrease (the ‘Synthetic-RZ⁻ chart’).

Designing the one-sided Synthetic-RZ-ME charts means fixing, for the lower-sided chart, the lower control limit LCL^- of its Shewhart-RZ sub-chart together with the limit H^- of its *CRL* sub-chart, and, for the upper-sided chart, the upper control limit UCL^+ together with the limit H^+ . The two charts are run according to the steps below:

- **Step 1.** Fix the target pair (H^-, LCL^-) for the lower-sided chart (or (H^+, UCL^+) for the upper-sided one).

- **Step 2.** At time i ($i = 1, 2, \dots$), draw a pair of random samples of size $n \times m$, written $(X_{i,j,k}^*, Y_{i,j,k}^*)$, and form the statistic \hat{Z}_i^* via (25).
- **Step 3.** If the sample conforms— $\hat{Z}_i^* < UCL^+$ for the upper-sided chart, or $\hat{Z}_i^* > LCL^-$ for the lower-sided chart—go back to Step 2 with time advanced to $i + 1$; otherwise continue to Step 4.
- **Step 4.** Evaluate the CRL and compare it against the CRL sub-chart limit (H^+ or H^-). If $CRL > H^+$ (or $CRL > H^-$), treat the process as in control and return to Step 2; otherwise proceed to Step 5.
- **Step 5.** Declare the process out of control, locate and eliminate the assignable cause, and then resume at Step 2.

4.3 Run length properties via the Markov chain approach

Chart performance is customarily judged by the average run length (ARL), the expected number of samples collected before the first out-of-control alarm; a smaller ARL signifies better detection. Our aim is thus to choose the control limits (H^{-*}, LCL^{-*}) or (H^{+*}, UCL^{+*}) so that, for a prescribed out-of-control scenario, the ARL is minimised while the in-control ARL is held at a preset level ARL_0 . The two one-sided design problems can be stated as follows:

- for the Synthetic-RZ⁻-ME chart,

$$(H^{-*}, LCL^{-*}) = \arg \min_{(H^-, LCL^-)} ARL(H^-, LCL^-, n, \gamma_{X^*}, \gamma_{Y^*}, \rho_0^*, \rho_1^*, \tau) \quad (31)$$

subject to

$$ARL(H^-, LCL^-, n, \gamma_{X^*}, \gamma_{Y^*}, \rho_0^*, \tau = 1) = ARL_0, \quad (32)$$

- for the Synthetic-RZ⁺-ME chart,

$$(H^{+*}, UCL^{+*}) = \arg \min_{(H^+, UCL^+)} ARL(H^+, UCL^+, n, \gamma_{X^*}, \gamma_{Y^*}, \rho_0^*, \rho_1^*, \tau) \quad (33)$$

subject to

$$ARL(H^+, UCL^+, n, \gamma_{X^*}, \gamma_{Y^*}, \rho_0^*, \tau = 1) = ARL_0. \quad (34)$$

We describe below how the ARL of the Synthetic-RZ⁻-ME chart is obtained; the Synthetic-RZ⁺-ME case follows along the same lines.

To derive the run-length properties of the Synthetic-RZ⁻-ME chart we adopt a Markov chain whose transition probability matrix \mathbf{P} is

$$\mathbf{P} = \begin{pmatrix} \mathbf{Q} & \mathbf{r} \\ \mathbf{0}^\top & \mathbf{1} \end{pmatrix} = \left(\begin{array}{cccc|c} 1-\theta & \theta & 0 & \dots & 0 & 0 \\ 0 & 0 & 1-\theta & & 0 & \theta \\ \vdots & & & \ddots & \vdots & \vdots \\ 0 & \dots & \dots & 0 & 1-\theta & \theta \\ \hline 1-\theta & 0 & \dots & \dots & 0 & \theta \\ 0 & \dots & \dots & \dots & 0 & 1 \end{array} \right),$$

in which \mathbf{Q} is the $(H^- + 1) \times (H^- + 1)$ sub-matrix governing transitions among the transient states, $\mathbf{0}^\top = (0, 0, \dots, 0)$ is a $1 \times (H^- + 1)$ row vector, \mathbf{r} is the $(H^- + 1) \times 1$ column vector with $\mathbf{r} = \mathbf{1} - \mathbf{Q}\mathbf{1}$ and $\mathbf{1} = (1, 1, \dots, 1)^\top$, and θ is the probability that a sample is nonconforming. Specifically,

- for the downward chart,

$$\theta = F_{\hat{Z}_i^*}(LCL^- | n, \gamma_{X^*}, \gamma_{Y^*}, z_1^*, \rho_1^*); \quad (35)$$

- for the upward chart,

$$\theta = 1 - F_{\hat{Z}_i^*}(UCL^+ | n, \gamma_{X^*}, \gamma_{Y^*}, z_1^*, \rho_1^*), \quad (36)$$

with $F_{\hat{Z}_i^*}(\dots)$ as in (29).

Letting $\mathbf{q} = (q_0, q_1, \dots, q_{H^-})^\top$ denote the $(H^- + 1) \times 1$ vector of initial probabilities over the transient states, the zero-state *ARL* is given by (see Davis and Woodall⁹)

$$ARL = \mathbf{q}^\top \mathbf{I} - \mathbf{Q}^{-1} \mathbf{1}. \quad (37)$$

In practice a process that has run in control for some time settles into a steady state, and the long-run behaviour of the chart is then better captured by the steady-state *ARL*. The Markov chain again furnishes the *cyclical* steady-state *ARL*:

$$ARL = \boldsymbol{\psi}^\top \mathbf{I} - \mathbf{Q}^{-1} \mathbf{1}, \quad (38)$$

in which the *cyclical* steady-state vector $\boldsymbol{\psi}$ is $\boldsymbol{\psi} = \frac{\mathbf{I} - (\mathbf{Q}^\top)^{-1} \mathbf{q}}{\mathbf{1}^\top \mathbf{I} - \mathbf{1}^\top (\mathbf{Q}^\top)^{-1} \mathbf{q}}$, as established by Darroch and Seneta⁸.

Frequently the exact shift size τ is unknown when the chart is designed, and in that event relying on the *ARL* as a performance measure may produce a poorly tuned chart. For this reason we also gauge performance by the expected average run length (*EARL*),

$$EARL = \int_{\Omega} ARL \times f_\tau(\tau) d\tau, \quad (39)$$

where $f_\tau(\tau)$ is the density of the random shift τ over a support Ω . In keeping with common SPC practice, τ is taken to be uniformly distributed on a chosen interval $[a, b]$ (see, for example, Nguyen et al.¹⁵), so that $f_\tau(\tau) = \frac{1}{b-a}$ for $\tau \in \Omega = [a, b]$. As in Tran et al.²⁷, two ranges are considered: $\Omega_D = [0.9, 1)$ for a decrease in τ and $\Omega_I = (1, 1.1]$ for an increase.

5 The effect of measurement error on the one-sided Synthetic-RZ control charts

This section reports how measurement error affects the two proposed charts. For convenience and without loss of generality, the in-control ratio and the target ARL are fixed at $z_0 = 1$ and $ARL_0 = 200$, respectively, and the mean shift of $Y_{i,j}$ is set to $\delta_Y = 1$. The remaining process parameters are allowed to vary over the following grid:

- $\gamma_X \in \{0.01, 0.2\}$, $\gamma_Y \in \{0.01, 0.2\}$,
- $n \in \{1, 5, 7, 10, 15\}$,
- $\rho_0 \in \{-0.8, -0.4, 0, 0.4, 0.8\}$,
- $\tau \in \Omega_D = [0.9, 1)$ for the Synthetic-RZ⁻-ME chart and $\tau \in \Omega_I = (1, 1.1]$ for the Synthetic-RZ⁺-ME chart.

5.1 Effect on the control limits

Table (1) lists the optimal couples (LCL^-, H^-) for the Synthetic-RZ⁻-ME chart together with (UCL^+, H^+) for the Synthetic-RZ⁺-ME chart, computed in the zero state with measurement error present and with $\theta_X = \theta_Y = 0.01$, $\eta_X = \eta_Y = 0.28$, $m = 1$, $\rho_M = 0.5$ and $ARL_0 = 200$. The analogous steady-state quantities appear in Table (2).

Two observations stand out. Although measurement error clearly alters the numerical values of the limits, the qualitative pattern matches what is seen when no error is present: both LCL^- and UCL^+ vary with n and with ρ_0 , and the reciprocal relationship $LCL^- \approx 1/UCL^+$ continues to hold whenever $\gamma_X = \gamma_Y$. In addition, introducing measurement error pushes the two limits farther apart and modifies H^- (respectively H^+); the larger the error, the wider the resulting interval between the limits.

γ_X	γ_Y	ρ_0	$n = 1$	$n = 5$	$n = 7$	$n = 10$	$n = 15$
0.01	0.01	-0.8	(0.9622, 14)	(0.9843, 6)	(0.9870, 5)	(0.9894, 4)	(0.9916, 3)
			(1.0393, 14)	(1.0159, 6)	(1.0132, 5)	(1.0107, 4)	(1.0084, 3)
0.01	0.01	-0.4	(0.9667, 13)	(0.9864, 5)	(0.9888, 4)	(0.9909, 3)	(0.9926, 3)
			(1.0342, 12)	(1.0138, 5)	(1.0113, 4)	(1.0091, 3)	(1.0075, 3)
0.01	0.01	0.0	(0.9721, 11)	(0.9887, 4)	(0.9908, 3)	(0.9923, 3)	(0.9940, 2)
			(1.0287, 11)	(1.0114, 4)	(1.0093, 3)	(1.0078, 3)	(1.0060, 2)
0.01	0.01	0.4	(0.9787, 8)	(0.9915, 3)	(0.9932, 2)	(0.9943, 2)	(0.9953, 2)
			(1.0217, 8)	(1.0086, 3)	(1.0069, 2)	(1.0058, 2)	(1.0047, 2)
0.01	0.01	0.8	(0.9876, 5)	(0.9950, 2)	(0.9958, 2)	(0.9965, 2)	(0.9974, 1)
			(1.0126, 5)	(1.0050, 2)	(1.0042, 2)	(1.0035, 2)	(1.0026, 1)
0.2	0.2	-0.8	(0.4704, 42)	(0.7280, 35)	(0.7662, 33)	(0.8015, 31)	(0.8354, 30)
			(1.8806, 7)	(1.3540, 20)	(1.2924, 21)	(1.2399, 22)	(1.1916, 22)
0.2	0.2	-0.4	(0.5129, 40)	(0.7559, 33)	(0.7905, 32)	(0.8226, 30)	(0.8536, 28)
			(1.7672, 8)	(1.3092, 21)	(1.2549, 21)	(1.2096, 22)	(1.1678, 22)
0.2	0.2	0.0	(0.5669, 38)	(0.7891, 31)	(0.8196, 30)	(0.8478, 28)	(0.8745, 27)
			(1.6454, 10)	(1.2575, 21)	(1.2139, 22)	(1.1756, 22)	(1.1409, 22)
0.2	0.2	0.4	(0.6428, 33)	(0.8312, 29)	(0.8562, 28)	(0.8792, 26)	(0.9011, 24)
			(1.4918, 12)	(1.1971, 21)	(1.1643, 22)	(1.1353, 22)	(1.1085, 21)
0.2	0.2	0.8	(0.7659, 27)	(0.8946, 24)	(0.9108, 23)	(0.9256, 21)	(0.9394, 19)
			(1.2861, 15)	(1.1164, 21)	(1.0967, 20)	(1.0797, 19)	(1.0642, 18)
0.01	0.2	-0.8	(0.7116, 42)	(0.8503, 32)	(0.8711, 30)	(0.8905, 28)	(0.9096, 25)
			(1.4939, 6)	(1.1988, 18)	(1.1641, 19)	(1.1338, 19)	(1.1067, 19)
0.01	0.2	-0.4	(0.7166, 42)	(0.8529, 32)	(0.8737, 29)	(0.8924, 28)	(0.9112, 25)
			(1.4853, 6)	(1.1953, 18)	(1.1612, 19)	(1.1315, 19)	(1.1049, 19)
0.01	0.2	0.0	(0.7217, 42)	(0.8558, 31)	(0.8760, 29)	(0.8946, 27)	(0.9128, 25)
			(1.4765, 6)	(1.1918, 18)	(1.1583, 19)	(1.1291, 19)	(1.1030, 19)
0.01	0.2	0.4	(0.7269, 42)	(0.8585, 31)	(0.8783, 29)	(0.8966, 27)	(0.9144, 25)
			(1.4676, 6)	(1.1882, 18)	(1.1553, 19)	(1.1267, 19)	(1.1010, 19)
0.01	0.2	0.8	(0.7323, 42)	(0.8613, 31)	(0.8807, 29)	(0.8986, 27)	(0.9163, 24)
			(1.4585, 6)	(1.1846, 18)	(1.1523, 19)	(1.1242, 19)	(1.0991, 19)
0.2	0.01	-0.8	(0.5455, 30)	(0.7967, 27)	(0.8285, 26)	(0.8564, 26)	(0.8834, 24)
			(1.4683, 29)	(1.2057, 26)	(1.1736, 26)	(1.1446, 25)	(1.1176, 24)
0.2	0.01	-0.4	(0.5511, 29)	(0.7995, 27)	(0.8310, 26)	(0.8590, 25)	(0.8852, 24)
			(1.4565, 29)	(1.2020, 27)	(1.1701, 26)	(1.1418, 25)	(1.1153, 24)
0.2	0.01	0.0	(0.5544, 30)	(0.8024, 27)	(0.8335, 26)	(0.8612, 25)	(0.8870, 24)
			(1.4459, 30)	(1.1976, 27)	(1.1665, 26)	(1.1389, 25)	(1.1130, 24)
0.2	0.01	0.4	(0.5603, 29)	(0.8054, 27)	(0.8361, 26)	(0.8634, 25)	(0.8893, 23)
			(1.4338, 30)	(1.1932, 27)	(1.1629, 26)	(1.1359, 25)	(1.1106, 24)
0.2	0.01	0.8	(0.5650, 29)	(0.8090, 26)	(0.8388, 26)	(0.8657, 25)	(0.8912, 23)
			(1.4217, 30)	(1.1887, 27)	(1.1592, 26)	(1.1329, 25)	(1.1082, 24)

Table 1: Optimal couples (LCL^- , H^-) (upper row) and (UCL^+ , H^+) (lower row) of the one-sided Synthetic-RZ-ME chart in the zero state, for $z_0 = 1$, $\theta_X = \theta_Y = 0.01$, $\eta_X = \eta_Y = 0.28$, $\rho_M = 0.5$, $m = 1$ and $ARL_0 = 200$.

γ_X	γ_Y	ρ_0	$n = 1$	$n = 5$	$n = 7$	$n = 10$	$n = 15$
0.01	0.01	-0.8	(0.9665, 5) (1.0346, 5)	(0.9858, 3) (1.0144, 3)	(0.9880, 3) (1.0122, 3)	(0.9899, 3) (1.0102, 3)	(0.9922, 2) (1.0079, 2)
0.01	0.01	-0.4	(0.9703, 5) (1.0306, 5)	(0.9874, 3) (1.0128, 3)	(0.9893, 3) (1.0108, 3)	(0.9915, 2) (1.0085, 2)	(0.9931, 2) (1.0070, 2)
0.01	0.01	0.0	(0.9747, 5) (1.0259, 5)	(0.9893, 3) (1.0108, 3)	(0.9914, 2) (1.0087, 2)	(0.9928, 2) (1.0072, 2)	(0.9941, 2) (1.0059, 2)
0.01	0.01	0.4	(0.9806, 4) (1.0198, 4)	(0.9920, 2) (1.0080, 2)	(0.9933, 2) (1.0068, 2)	(0.9944, 2) (1.0057, 2)	(0.9950, 4) (1.0051, 4)
0.01	0.01	0.8	(0.9885, 3) (1.0116, 3)	(0.9948, 3) (1.0052, 3)	(0.9949, 13) (1.0051, 12)	(0.9956, 17) (1.0044, 17)	(0.9964, 18) (1.0036, 18)
0.2	0.2	-0.8	(0.5723, 3) (1.6941, 2)	(0.7773, 4) (1.2754, 3)	(0.8085, 4) (1.2278, 3)	(0.8335, 5) (1.1870, 3)	(0.8619, 5) (1.1558, 4)
0.2	0.2	-0.4	(0.6096, 3) (1.5959, 2)	(0.8001, 4) (1.2402, 3)	(0.8245, 5) (1.1991, 3)	(0.8511, 5) (1.1701, 4)	(0.8768, 5) (1.1367, 4)
0.2	0.2	0.0	(0.6559, 3) (1.4892, 2)	(0.8273, 4) (1.2009, 3)	(0.8487, 5) (1.1734, 4)	(0.8720, 5) (1.1429, 4)	(0.8943, 5) (1.1151, 4)
0.2	0.2	0.4	(0.7085, 4) (1.3676, 2)	(0.8584, 5) (1.1604, 4)	(0.8792, 5) (1.1337, 4)	(0.8981, 5) (1.1105, 4)	(0.9161, 5) (1.0916, 5)
0.2	0.2	0.8	(0.8094, 4) (1.2257, 3)	(0.9108, 5) (1.0954, 4)	(0.9242, 5) (1.0820, 5)	(0.9351, 6) (1.0680, 5)	(0.9468, 6) (1.0551, 5)
0.01	0.2	-0.8	(0.7543, 5) (1.3976, 2)	(0.8736, 5) (1.1560, 3)	(0.8911, 5) (1.1340, 4)	(0.9056, 6) (1.1098, 4)	(0.9216, 6) (1.0879, 4)
0.01	0.2	-0.4	(0.7586, 5) (1.3906, 2)	(0.8758, 5) (1.1533, 3)	(0.8911, 6) (1.1317, 4)	(0.9072, 6) (1.1079, 4)	(0.9230, 6) (1.0864, 4)
0.01	0.2	0.0	(0.7629, 5) (1.3836, 2)	(0.8780, 5) (1.1505, 3)	(0.8930, 6) (1.1293, 4)	(0.9089, 6) (1.1059, 4)	(0.9244, 6) (1.0848, 4)
0.01	0.2	0.4	(0.7674, 5) (1.3764, 2)	(0.8803, 5) (1.1477, 3)	(0.8950, 6) (1.1268, 4)	(0.9106, 6) (1.1039, 4)	(0.9258, 6) (1.0832, 4)
0.01	0.2	0.8	(0.7719, 5) (1.3691, 2)	(0.8826, 5) (1.1448, 3)	(0.8971, 6) (1.1244, 4)	(0.9124, 6) (1.1019, 4)	(0.9272, 6) (1.0816, 4)
0.2	0.01	-0.8	(0.6448, 3) (1.3643, 3)	(0.8344, 4) (1.1675, 4)	(0.8599, 4) (1.1415, 4)	(0.8797, 5) (1.1213, 5)	(0.9017, 5) (1.0990, 5)
0.2	0.01	-0.4	(0.6489, 3) (1.3558, 3)	(0.8369, 4) (1.1641, 4)	(0.8620, 4) (1.1387, 4)	(0.8816, 5) (1.1190, 5)	(0.9033, 5) (1.0971, 5)
0.2	0.01	0.0	(0.6530, 3) (1.3471, 3)	(0.8393, 4) (1.1607, 4)	(0.8642, 4) (1.1358, 4)	(0.8835, 5) (1.1166, 5)	(0.9048, 5) (1.0952, 5)
0.2	0.01	0.4	(0.6573, 3) (1.3384, 3)	(0.8419, 4) (1.1572, 4)	(0.8664, 4) (1.1329, 4)	(0.8854, 5) (1.1141, 5)	(0.9065, 5) (1.0932, 5)
0.2	0.01	0.8	(0.6617, 3) (1.3296, 3)	(0.8444, 4) (1.1537, 4)	(0.8687, 4) (1.1333, 5)	(0.8874, 5) (1.1116, 5)	(0.9081, 5) (1.0912, 5)

Table 2: Values of (LCL^-, H^-) (first row) and (UCL^+, H^+) (second row) for the one-sided Synthetic-RZ-ME chart in steady state, with $z_0 = 1$, $\theta_X = \theta_Y = 0.01$, $\eta_X = \eta_Y = 0.28$, $\rho_M = 0.5$, $m = 1$, $ARL_0 = 200$.

5.2 Effect on the chart performance

To assess detection capability, Tables (3)–(6) collect the $EARL$ values obtained under two run-length scenarios—the zero-state case (Tables (3)–(4)) and the steady-state case (Tables (5)–(6))—and for two settings of the correlation, namely $\rho_0 = \rho_1$ (Tables (3) and (5)) and $\rho_1 = -0.8 \neq \rho_0$ (Tables (4) and (6)).

The tabulated figures point to two findings of practical relevance. On the one hand, enlarging the sample from $n = 1$ to $n = 15$ lowers *EARL* by a factor of roughly two to three for every parameter combination examined, so increasing the sample size remains the single most powerful lever for sharpening detection. On the other hand, the steady-state values exceed their zero-state counterparts by about 15–20%; this gap agrees with a familiar feature of synthetic schemes and provides a useful internal check on the Markov-chain computations.

γ_X	γ_Y	ρ_0	$n = 1$	$n = 5$	$n = 7$	$n = 10$	$n = 15$
0.01	0.01	-0.8	4.3	1.5	1.3	1.1	1.1
			4.3	1.4	1.3	1.1	1.1
0.01	0.01	-0.4	3.6	1.3	1.2	1.1	1.0
			3.5	1.3	1.2	1.1	1.0
0.01	0.01	0.0	2.8	1.2	1.1	1.1	1.0
			2.7	1.2	1.1	1.0	1.0
0.01	0.01	0.4	2.0	1.1	1.0	1.0	1.0
			1.9	1.1	1.0	1.0	1.0
0.01	0.01	0.8	1.2	1.0	1.0	1.0	1.0
			1.2	1.0	1.0	1.0	1.0
0.2	0.2	-0.8	85.9	50.8	44.0	37.4	30.7
			120.5	61.4	51.6	42.6	33.8
0.2	0.2	-0.4	81.2	45.9	39.5	33.3	27.0
			111.7	54.4	45.4	37.2	29.3
0.2	0.2	0.0	74.7	39.8	33.9	28.2	22.6
			99.9	45.8	38.0	30.8	24.0
0.2	0.2	0.4	64.5	31.6	26.4	21.6	16.9
			82.6	35.0	28.6	22.9	17.5
0.2	0.2	0.8	44.4	18.3	14.8	11.6	8.7
			52.0	19.2	15.2	11.8	8.7
0.01	0.2	-0.8	53.4	27.6	23.2	19.1	15.0
			88.6	35.7	28.9	22.8	17.3
0.01	0.2	-0.4	52.5	27.0	22.7	18.6	14.6
			87.6	35.0	28.3	22.4	16.9
0.01	0.2	0.0	51.7	26.4	22.2	18.2	14.3
			86.5	34.3	27.7	21.9	16.5
0.01	0.2	0.4	50.8	25.9	21.7	17.8	13.9
			85.4	33.7	27.1	21.4	16.1
0.01	0.2	0.8	49.9	25.3	21.2	17.3	13.5
			84.2	33.0	26.5	20.9	15.7
0.2	0.01	-0.8	78.1	38.6	32.3	26.5	20.8
			75.3	36.2	30.2	24.7	19.3
0.2	0.01	-0.4	77.5	38.1	31.8	26.0	20.4
			73.8	35.5	29.5	24.1	18.8
0.2	0.01	0.0	77.0	37.5	31.3	25.5	20.0
			72.4	34.7	28.9	23.5	18.4
0.2	0.01	0.4	76.4	36.9	30.8	25.1	19.5
			70.9	33.8	28.2	22.9	17.9
0.2	0.01	0.8	75.7	36.3	30.2	24.6	19.1
			69.4	33.0	27.4	22.3	17.4

Table 3: *EARL* of the Synthetic-RZ⁻-ME chart with $\tau \in \Omega_D = [0.9, 1)$ (first row) and Synthetic-RZ⁺-ME chart with $\tau \in \Omega_I = (1, 1.1]$ (second row) for $\rho_0 = \rho_1$, zero state.

γ_X	γ_Y	ρ_0	$n = 1$	$n = 5$	$n = 7$	$n = 10$	$n = 15$
0.01	0.01	-0.8	4.3	1.5	1.3	1.1	1.1
			4.3	1.4	1.3	1.1	1.1
0.01	0.01	-0.4	2.8	1.3	1.2	1.1	1.0
			2.7	1.3	1.2	1.1	1.0
0.01	0.01	0.0	1.9	1.2	1.1	1.1	1.0
			1.9	1.2	1.1	1.1	1.0
0.01	0.01	0.4	1.5	1.1	1.1	1.0	1.0
			1.5	1.1	1.1	1.0	1.0
0.01	0.01	0.8	1.2	1.1	1.0	1.0	1.0
			1.2	1.1	1.0	1.0	1.0
0.2	0.2	-0.8	85.9	50.8	44.0	37.4	30.7
			120.5	61.4	51.6	42.6	33.8
0.2	0.2	-0.4	38.1	22.4	19.7	17.1	14.3
			52.9	25.7	22.0	18.6	15.2
0.2	0.2	0.0	17.6	10.9	9.8	8.6	7.4
			21.8	11.6	10.3	9.0	7.6
0.2	0.2	0.4	8.4	5.7	5.2	4.7	4.1
			8.9	5.8	5.3	4.7	4.1
0.2	0.2	0.8	3.9	3.0	2.8	2.6	2.3
			3.8	3.0	2.8	2.5	2.3
0.01	0.2	-0.8	53.4	27.6	23.2	19.1	15.0
			88.6	35.7	28.9	22.8	17.3
0.01	0.2	-0.4	44.2	23.8	20.2	16.7	13.2
			80.7	31.8	25.7	20.4	15.5
0.01	0.2	0.0	36.9	20.7	17.6	14.7	11.7
			73.4	28.4	23.0	18.2	13.9
0.01	0.2	0.4	31.1	18.0	15.5	13.0	10.4
			66.8	25.3	20.5	16.3	12.5
0.01	0.2	0.8	26.4	15.8	13.6	11.5	9.3
			60.6	22.6	18.4	14.6	11.2
0.2	0.01	-0.8	78.1	38.6	32.3	26.5	20.8
			75.3	36.2	30.2	24.7	19.3
0.2	0.01	-0.4	71.6	34.6	28.9	23.7	18.6
			60.9	30.9	26.0	21.4	16.9
0.2	0.01	0.0	65.7	31.0	25.9	21.2	16.7
			49.6	26.5	22.4	18.6	14.8
0.2	0.01	0.4	60.2	27.9	23.3	19.1	15.0
			40.7	22.8	19.4	16.2	13.0
0.2	0.01	0.8	55.1	25.0	20.9	17.1	13.5
			33.7	19.7	16.9	14.2	11.5

Table 4: *EARL* for $\rho_1 = -0.8 \neq \rho_0$, zero state.

γ_X	γ_Y	ρ_0	$n = 1$	$n = 5$	$n = 7$	$n = 10$	$n = 15$
0.01	0.01	-0.8	6.2	2.6	2.3	2.1	2.0
			6.1	2.5	2.3	2.1	2.0
0.01	0.01	-0.4	5.3	2.4	2.2	2.1	2.0
			5.2	2.3	2.1	2.0	2.0
0.01	0.01	0.0	4.3	2.2	2.1	2.0	1.9
			4.2	2.2	2.1	2.0	1.9
0.01	0.01	0.4	3.3	2.0	2.0	1.9	1.9
			3.2	2.0	2.0	1.9	1.9
0.01	0.01	0.8	2.2	1.9	1.7	1.7	1.7
			2.2	1.9	1.8	1.7	1.7
0.2	0.2	-0.8	98.1	59.0	51.6	43.9	36.3
			124.5	68.2	58.3	48.7	39.1
0.2	0.2	-0.4	92.8	53.6	46.2	39.2	32.1
			116.3	61.0	51.6	42.7	34.1
0.2	0.2	0.0	85.5	46.8	39.9	33.5	27.1
			105.2	52.1	43.5	35.8	28.3
0.2	0.2	0.4	73.5	37.3	31.4	26.0	20.7
			88.6	40.3	33.3	27.1	21.1
0.2	0.2	0.8	51.3	22.2	18.2	14.6	11.3
			57.8	22.9	18.5	14.7	11.2
0.01	0.2	-0.8	62.6	33.0	28.0	23.2	18.6
			93.2	40.8	33.4	26.9	20.8
0.01	0.2	-0.4	61.7	32.4	27.4	22.8	18.2
			92.2	40.1	32.8	26.3	20.3
0.01	0.2	0.0	60.8	31.8	26.9	22.3	17.8
			91.1	39.4	32.2	25.8	19.9
0.01	0.2	0.4	59.8	31.1	26.3	21.8	17.4
			90.0	38.6	31.5	25.3	19.5
0.01	0.2	0.8	58.8	30.5	25.7	21.3	16.9
			88.9	37.9	30.9	24.7	19.0
0.2	0.01	-0.8	87.4	45.0	38.0	31.4	25.0
			84.1	42.1	35.5	29.2	23.2
0.2	0.01	-0.4	86.8	44.3	37.4	30.8	24.5
			82.7	41.3	34.7	28.6	22.7
0.2	0.01	0.0	86.1	43.7	36.8	30.3	24.0
			81.3	40.4	34.0	27.9	22.1
0.2	0.01	0.4	85.3	43.0	36.2	29.7	23.6
			79.8	39.5	33.2	27.3	21.6
0.2	0.01	0.8	84.6	42.3	35.5	29.2	23.1
			78.3	38.6	32.3	26.6	21.1

Table 5: *EARL* for $\rho_0 = \rho_1$, steady state.

γ_X	γ_Y	ρ_0	$n = 1$	$n = 5$	$n = 7$	$n = 10$	$n = 15$
0.01	0.01	-0.8	6.2	2.6	2.3	2.1	2.0
			6.1	2.5	2.3	2.1	2.0
0.01	0.01	-0.4	4.4	2.3	2.2	2.1	2.0
			4.3	2.3	2.1	2.1	2.0
0.01	0.01	0.0	3.3	2.2	2.1	2.0	2.0
			3.3	2.2	2.1	2.0	1.9
0.01	0.01	0.4	2.7	2.1	2.0	2.0	1.9
			2.7	2.1	2.0	2.0	1.9
0.01	0.01	0.8	2.3	2.0	1.8	1.7	1.7
			2.3	2.0	1.8	1.7	1.7
0.2	0.2	-0.8	98.1	59.0	51.6	43.9	36.3
			124.5	68.2	58.3	48.7	39.1
0.2	0.2	-0.4	53.9	32.0	27.7	24.0	20.2
			67.5	36.5	31.6	26.2	21.5
0.2	0.2	0.0	28.9	17.6	15.3	13.5	11.6
			35.5	19.7	16.6	14.4	12.2
0.2	0.2	0.4	14.3	9.5	8.7	7.8	6.9
			18.0	10.1	9.1	8.1	6.9
0.2	0.2	0.8	6.9	5.2	4.8	4.4	4.1
			7.5	5.3	4.8	4.5	4.1
0.01	0.2	-0.8	62.6	33.0	28.0	23.2	18.6
			93.2	40.8	33.4	26.9	20.8
0.01	0.2	-0.4	54.9	29.7	25.2	21.1	16.9
			86.5	37.6	30.7	24.7	19.1
0.01	0.2	0.0	48.3	26.8	22.8	19.1	15.5
			80.3	34.5	28.2	22.7	17.6
0.01	0.2	0.4	42.5	24.2	20.6	17.4	14.1
			74.5	31.8	25.9	20.9	16.3
0.01	0.2	0.8	37.6	21.9	18.7	15.9	13.0
			69.0	29.2	23.8	19.2	15.0
0.2	0.01	-0.8	87.4	45.0	38.0	31.4	25.0
			84.1	42.1	35.5	29.2	23.2
0.2	0.01	-0.4	81.6	41.4	35.0	28.8	23.0
			73.4	37.7	31.9	26.3	21.0
0.2	0.01	0.0	76.2	38.1	32.2	26.5	21.2
			64.2	33.7	28.7	23.7	19.1
0.2	0.01	0.4	71.0	35.1	29.6	24.4	19.5
			56.3	30.3	25.9	21.4	17.3
0.2	0.01	0.8	66.2	32.3	27.3	22.4	18.0
			49.4	27.2	23.0	19.4	15.8

Table 6: *EARL* for $\rho_1 = -0.8 \neq \rho_0$, steady state.

5.2.1 Effect of precision errors η_X and η_Y

We first turn to the precision component of the error, captured by η_X and η_Y . Holding $\gamma_X = \gamma_Y \in \{0.01, 0.2\}$, $\rho_M = 0$ and $\theta_X = \theta_Y = 0$, we treat two correlation configurations, $\rho_0 = \rho_1 = -0.8$ and $\rho_0 = -0.4$, $\rho_1 = -0.8$, and let each of η_X and η_Y range over $\{0, 0.1, 0.2, \dots, 1\}$. The resulting *EARL*

curves are displayed in Figures 1–2.

Because $EARL$ grows as η_X and η_Y increase, the precision error evidently harms the charts. To illustrate, with $n = 1$, $\Omega_I = (1, 1.1]$, $\rho_0 = \rho_1 = -0.8$ and $\gamma_X = \gamma_Y = 0.2$, the chart yields $EARL = 27.8$ at $\eta_X = \eta_Y = 0.1$, and a still larger value once $\eta_X = \eta_Y = 1$. The deterioration is nevertheless modest as long as the precision error stays small. Raising n again helps substantially: across the whole range, the $EARL$ obtained for $n = 15$ never exceeds that for $n = 1$, whether or not measurement error is present.

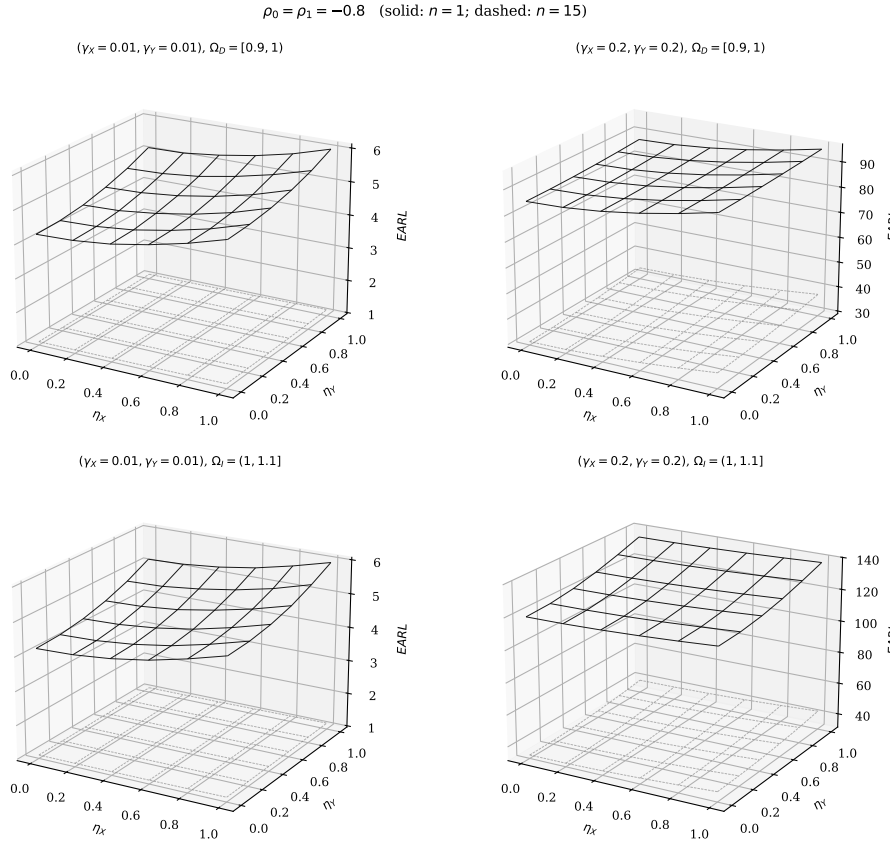


Figure 1: Behaviour of $EARL$ as a function of the precision errors η_X and η_Y , with $\theta_X = \theta_Y = 0$, $\rho_M = 0$, $n \in \{1, 15\}$, $\gamma_X = \gamma_Y \in \{0.01, 0.2\}$ and $\rho_0 = \rho_1 = -0.8$.

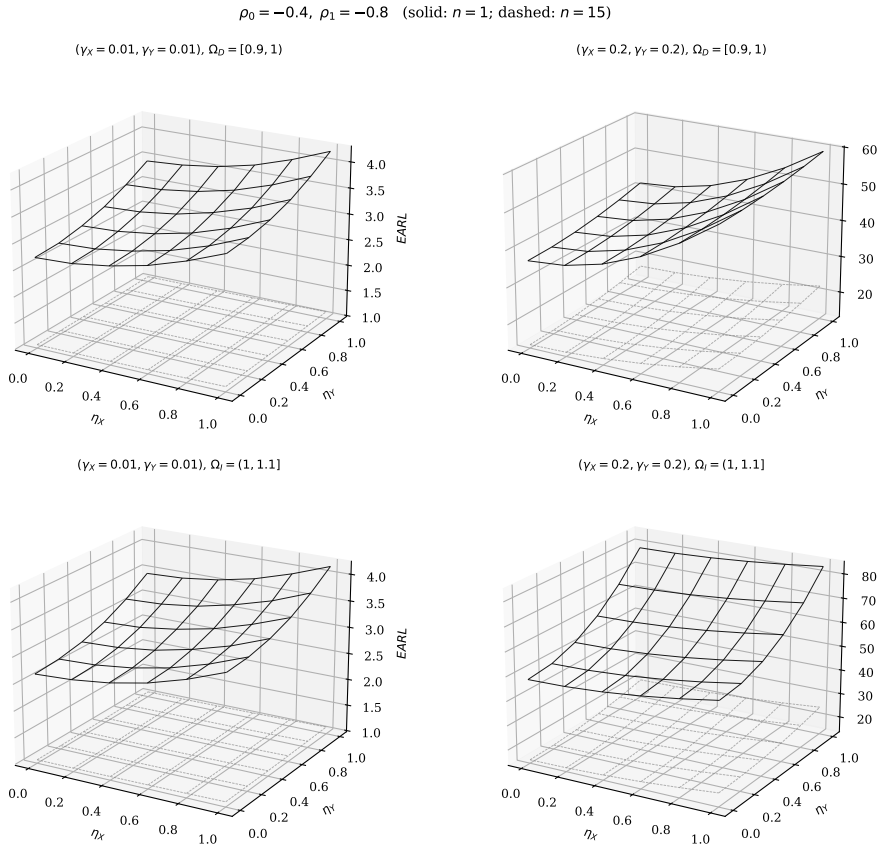


Figure 2: Behaviour of $EARL$ versus η_X and η_Y under the same configuration, but with $\rho_0 = -0.4$ and $\rho_1 = -0.8$.

5.2.2 Effect of accuracy errors θ_X and θ_Y

Next we consider the accuracy component, described by θ_X and θ_Y . We let both quantities vary over $\{0, 0.01, 0.02, \dots, 0.05\}$ while keeping $\gamma_X = \gamma_Y \in \{0.01, 0.2\}$, $\rho_M = 0$ and $\eta_X = \eta_Y = 0$, again under $\rho_0 = \rho_1 = -0.8$ (Figure 3) and $\rho_0 = -0.4, \rho_1 = -0.8$ (Figure 4).

The figures reveal that how θ_X and θ_Y act on $EARL$ is governed by the values of ρ_0 and ρ_1 . When $\rho_0 = \rho_1 = -0.8$, $EARL$ rises as θ_X increases and θ_Y decreases (Figure 3). The opposite pattern emerges for $\rho_0 = -0.4, \rho_1 = -0.8$, where $EARL$ climbs when θ_X falls and θ_Y rises. As before, a larger n markedly enhances performance, the $n = 15$ curves lying everywhere below the $n = 1$ curves irrespective of measurement error.

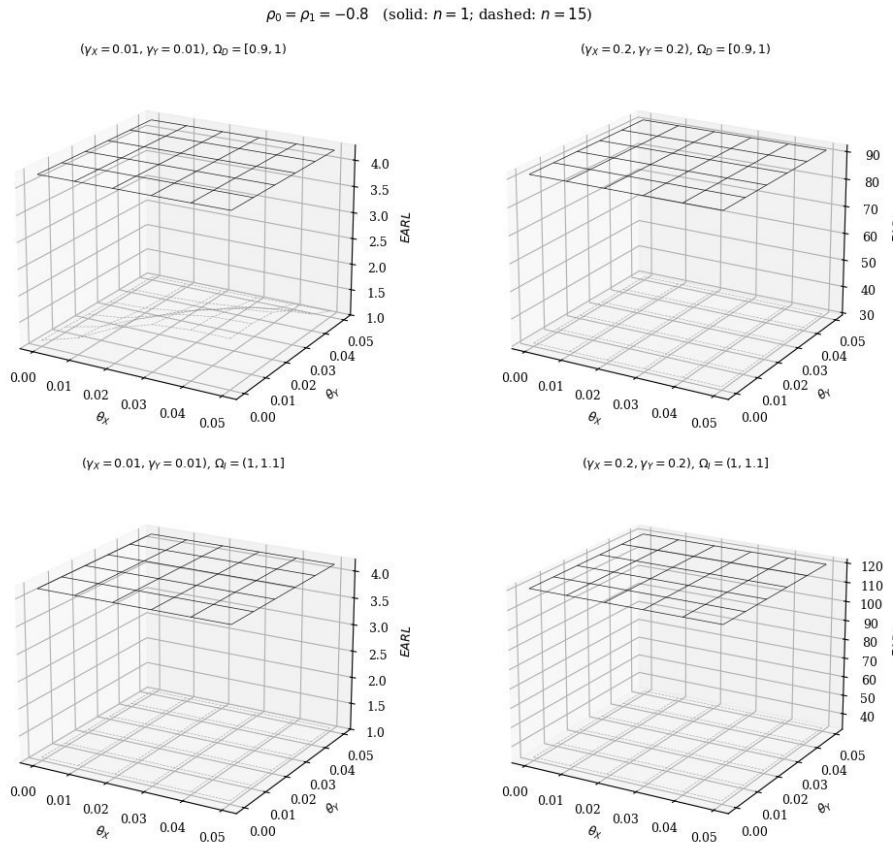


Figure 3: Influence of the accuracy errors θ_X and θ_Y on $EARL$ for $\eta_X = \eta_Y = 0$, $\rho_M = 0$ and $\rho_0 = \rho_1 = -0.8$.

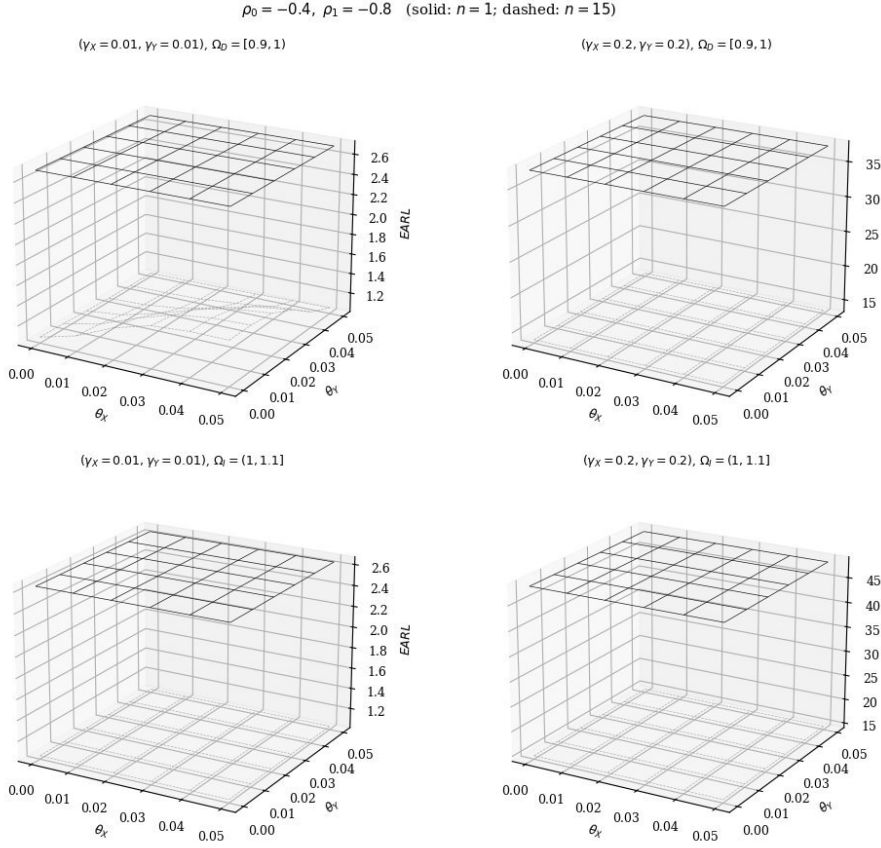


Figure 4: Influence of θ_X and θ_Y on $EARL$ for $\rho_0 = -0.4$ and $\rho_1 = -0.8$.

5.2.3 Effect of the measurement-error correlation ρ_M

The role of ρ_M is depicted in Figure 5 ($\rho_0 = \rho_1 = -0.8$) and Figure 6 ($\rho_0 = -0.4, \rho_1 = -0.8$), obtained with $\gamma_X = \gamma_Y \in \{0.01, 0.2\}$, $\theta_X = \theta_Y = 0.05$, $\eta_X = \eta_Y = 0.28$ and ρ_M ranging over $\{-1, -0.9, \dots, 0.9, 1\}$. The curves indicate that $EARL$ responds smoothly to ρ_M . With both ρ_0 and ρ_1 negative, a higher ρ_M produces a slight rise in $EARL$: a positive correlation between the measurement errors offsets part of the negative correlation in the process, so the standardized ratio becomes less concentrated and the chart loses a little of its sensitivity. The take-away is subtle yet practically relevant—the direction in which ρ_M acts hinges on the signs of ρ_0 and ρ_1 , and it would be a mistake to presume that mutually uncorrelated measurement errors invariably represent the least favourable situation.

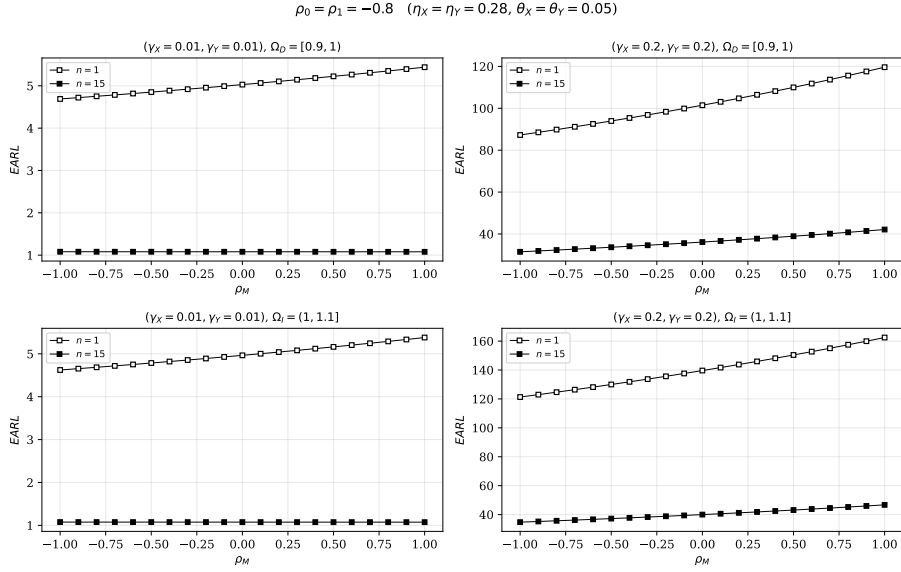


Figure 5: Dependence of $EARL$ on ρ_M for $\eta_X = \eta_Y = 0.28, \theta_X = \theta_Y = 0.05$ and $\rho_0 = \rho_1 = -0.8$.

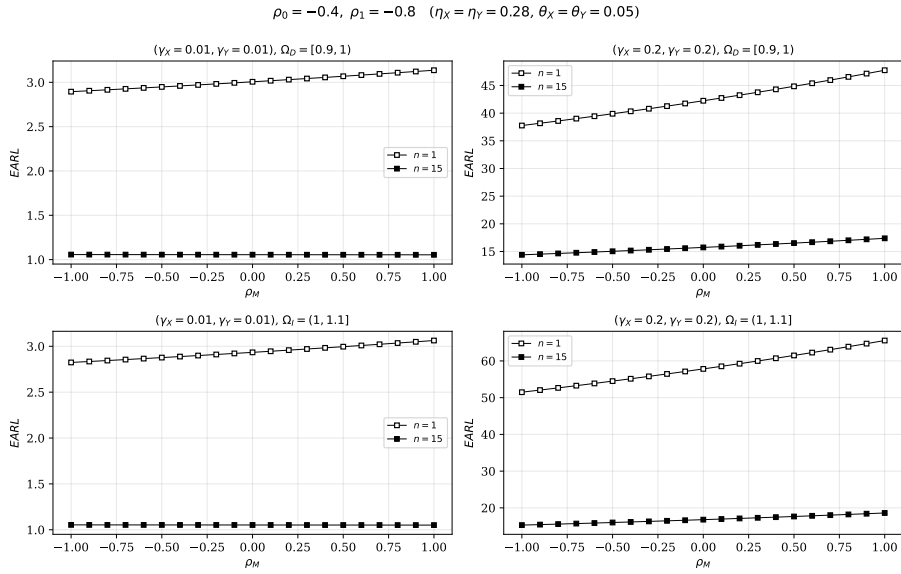


Figure 6: Dependence of $EARL$ on ρ_M for $\rho_0 = -0.4$ and $\rho_1 = -0.8$.

5.2.4 Effect of multiple measurements m

A recurring suggestion in the literature is that recording several measurements on each unit can offset the damage measurement error does to a chart. To test whether this holds for the Synthetic-RZ-ME chart, we evaluate

$EARL$ as m grows from 1 to 10, with $\gamma_X = \gamma_Y \in \{0.01, 0.2\}$, $\theta_X = \theta_Y = 0.05$ and $\eta_X = \eta_Y = 0.28$. Figures 7–8 report the outcome.

The conclusion is striking: enlarging m brings no appreciable gain in the performance of the Synthetic-RZ-ME chart—the curves in the figures stay almost flat. This mirrors the result reported by Tran et al.²⁷ for the Shewhart-RZ chart. Consequently, repeated measurement of each item is not a worthwhile strategy for mitigating the adverse effect of measurement error on these charts. From a practical standpoint the message is valuable: effort is better spent on shrinking the intrinsic measurement error itself—that is, on lowering η_X , η_Y , θ_X and θ_Y —than on accumulating repeated readings.

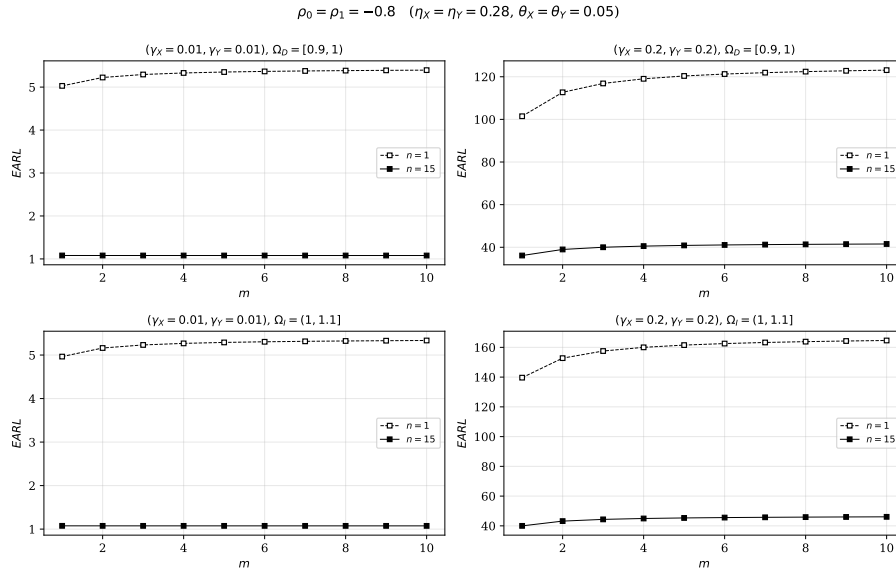


Figure 7: Effect of the number of repeated measurements m on $EARL$ for $\eta_X = \eta_Y = 0.28$, $\theta_X = \theta_Y = 0.05$ and $\rho_0 = \rho_1 = -0.8$.

$$\rho_0 = -0.4, \rho_1 = -0.8 \quad (\eta_X = \eta_Y = 0.28, \theta_X = \theta_Y = 0.05)$$

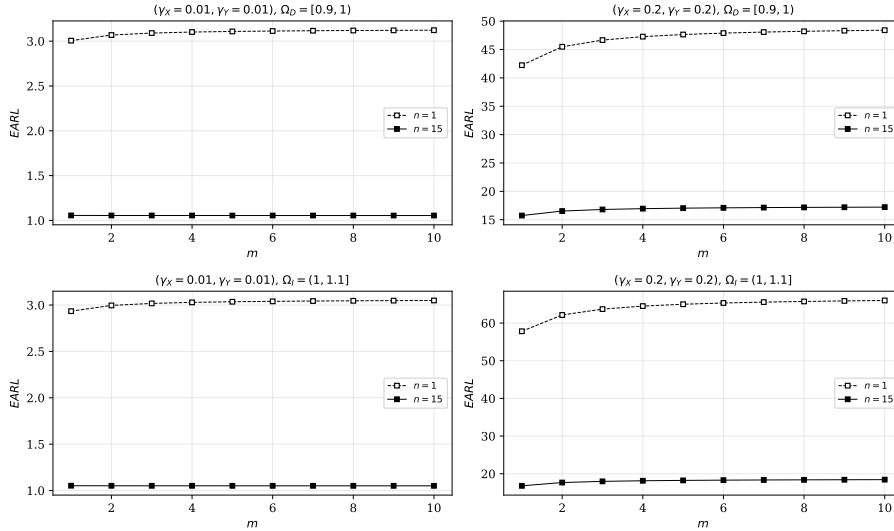


Figure 8: Effect of m on $EARL$ for $\rho_0 = -0.4$ and $\rho_1 = -0.8$.

5.3 Comparison with the Shewhart-RZ-ME chart

To bring out the merit of the proposed charts, we set their performance against that of the Shewhart-RZ-ME chart studied by Tran et al.²⁷. The comparison is admittedly not on an entirely level footing, since the two works rest on slightly different versions of the linear covariate error model and involve different chart families; even so, the Synthetic-RZ-ME charts are found to be markedly superior at picking up small-to-moderate shifts, particularly when the in-control configuration permits the Synthetic chart to operate with larger H^- or H^+ . This accords with the well-documented fact that Synthetic schemes usually detect shifts more effectively than Shewhart schemes. As an added benefit, the one-sided construction frees the Synthetic-RZ-ME charts from the ARL -biased behaviour that afflicts the two-sided Synthetic-RZ chart of Celano and Castagliola³.

6 Illustrative example

This section walks through an application of the one-sided Synthetic-RZ-ME chart under measurement error. We revisit the real waste-battery management problem at Italian battery-recycling plants previously considered by Tran et al.²⁷.

At the outset of recycling, batteries arrive at collection sites and are placed in dedicated drums, sacks or boxes, collectively called “batches”. Such batches often contain discarded items that are not recyclable batteries—small electronic devices, scrap metal and assorted waste—and removing this

material is necessary to contain recycling costs. The plant monitors the ratio Z of the recyclable-battery weight (denoted X) to the total batch weight (denoted Y) in order to quantify that cost. As in Tran et al.²⁷, the in-control ratio of interest, beyond which an economic loss is incurred, is set at $z_0 = 0.95$.

Samples of size $n = 5$ are taken at regular times $i = 1, 2, \dots$, the batches having a nominal weight of 100 kg. To reflect natural variability the batch weight is modelled as $Y \sim N(100, 1)$, and the recyclable-battery weight within a batch is likewise normal with mean $\mu_X = 95$ kg. At each time the sample mean weights $\bar{X}_i^* = \frac{1}{n} \sum_{j=1}^n X_{i,j}^*$ and $\bar{Y}_i^* = \frac{1}{n} \sum_{j=1}^n Y_{i,j}^*$ are recorded. The coefficients of variation are $\gamma_X = \gamma_Y = 0.01$ and the in-control correlation is $\rho_0 = 0.8$.

The linear covariate error model is assigned the parameters $\theta_X = \theta_Y = 0$, $\eta_X = \eta_Y = 0.28$, $\rho_1 = 0.8$ and $\rho_M = 0$. From sample #11 onward we simulate a downward shift amounting to at most 1% of the in-control ratio z_0 . For these values the optimal limit of the Synthetic-RZ⁻-ME chart is obtained by the procedure of Section 4. Figure 9 shows the resulting chart. It signals an out-of-control condition at sample #13—the plotted point falls below LCL^- and the associated CRL satisfies $CRL \leq H^-$ —suggesting that an assignable cause has shifted the process out of control. The conclusion coincides with that of Tran et al.²⁷.

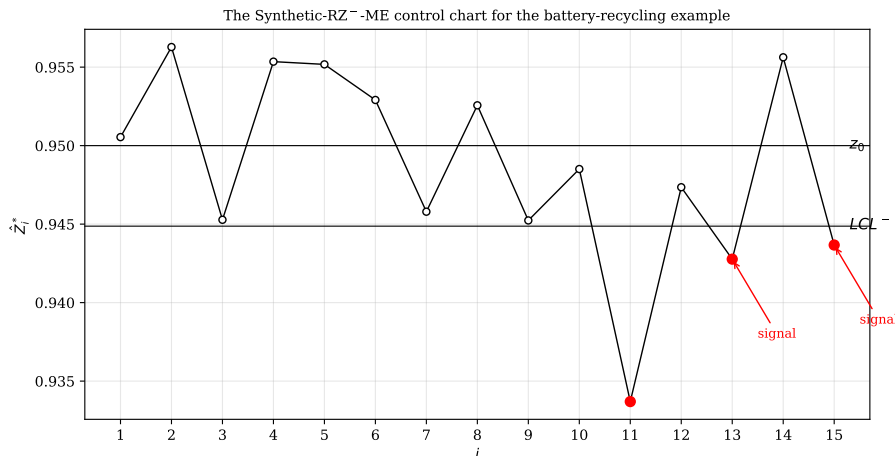


Figure 9: Application of the Synthetic-RZ⁻-ME chart, under measurement error, to the battery-recycling dataset.

7 Concluding remarks

This paper has examined how measurement error affects two one-sided Synthetic-RZ control charts used to monitor the ratio of two normal variables. The error was represented by a linear covariate error model, and we

derived in full how the model parameters shift from the in-control to the out-of-control state without resorting to the restrictive assumption that the shift size is independent of the measurement error. The run-length properties of the Synthetic-RZ-ME charts were computed through a Markov chain approach covering both the zero-state and the steady-state *ARL*.

The numerical evidence confirms that measurement error degrades the performance of the one-sided Synthetic-RZ-ME charts. The precision errors (η_X and η_Y) inflate the *EARL*, with larger errors producing worse detection. The accuracy errors (θ_X and θ_Y) act in a more intricate fashion that is contingent on the values of ρ_0 and ρ_1 . The correlation ρ_M between the measurement errors of X and Y works in the opposite direction: a larger ρ_M improves the chart. Enlarging the sample size n enhances performance considerably in every case, irrespective of measurement error.

A noteworthy outcome is that collecting several measurements per item ($m > 1$) does not effectively curb the harm measurement error does to the Synthetic-RZ-ME chart. This matches the conclusion reached for the Shewhart-RZ chart by Tran et al.²⁷ and constitutes a handy guideline for quality practitioners.

Several avenues remain open for further work. One is to attenuate the effect of measurement error by coupling the Synthetic-RZ chart with adaptive mechanisms such as variable sampling interval (VSI) or variable sample size (VSS), or with run rules. Another is to design other Synthetic-type charts—for instance Synthetic-EWMA-RZ or Synthetic-CUSUM-RZ—in the presence of measurement error. A final direction is to broaden the study to the monitoring of a multivariate ratio.

References

- [1] D. Brook and D.A. Evans. An approach to the probability distribution of CUSUM run length. *Biometrika*, 59(3):539–549, 1972.
- [2] A. Cedilnik, K. Kosmelj, and A. Blejec. The Distribution of the Ratio of Jointly Normal Variables. *Metodoloski Zvezki*, 1(1):99–108, 2004.
- [3] G. Celano and P. Castagliola. A Synthetic Control Chart for Monitoring the Ratio of Two Normal Variables. *Quality and Reliability Engineering International*, 32(2):681–696, 2016.
- [4] G. Celano and P. Castagliola. Design of a phase II Control Chart for Monitoring the Ratio of two Normal Variables. *Quality and Reliability Engineering International*, 32(1):291–308, 2016.
- [5] G. Celano, P. Castagliola, A. Faraz, and S. Fichera. Statistical Performance of a Control Chart for Individual Observations Monitoring

- the Ratio of two Normal Variables. *Quality and Reliability Engineering International*, 30(8):1361–1377, 2014.
- [6] X.B. Cheng and F. K. Wang. The performance of EWMA median and cusum median control charts for a normal process with measurement errors. *Quality and Reliability Engineering International*, 2017. DOI: 10.1002/qre.2248 (to appear).
 - [7] A.F.B. Costa and M.A. Rahim. A Synthetic Control Chart for Monitoring the Process Mean and Variance. *Journal of Quality in Maintenance Engineering*, 12(1):81–88, 2006.
 - [8] J.N. Darroch and E. Seneta. On quasi-stationary distributions in absorbing discrete-time finite markov chains. *Journal of Applied Probability*, 2(1):88–100, 1965.
 - [9] R.B. Davis and W.H. Woodall. Evaluating and Improving the Synthetic Control Chart. *Journal of Quality Technology*, 34(2):200–208, 2002.
 - [10] R.C. Geary. The Frequency Distribution of the Quotient of Two Normal Variates. *Journal of the Royal Statistical Society*, 93(3):442–446, 1930.
 - [11] J. Hayya, D. Armstrong, and N. Gressis. A note on the Ratio of Two Normally Distributed Variables. *Management Science*, 21(11):1338–1341, 1975.
 - [12] J.S Hunter. The Exponentially Weighted Moving Average. *Journal of Quality Technology*, 18:203–210, 1986.
 - [13] K.W. Linna and W.H. Woodall. Effect of measurement error on shewart control chart. *Jornal of Quality Technology*, 33(2):213–222, 2001.
 - [14] K.W. Linna, W.H. Woodall, and K.L. Busby. The performance of multivariate control charts in the presence of measurement error. *Journal of Quality Technology*, 33(3):349, 2001.
 - [15] H.D. Nguyen, K.P. Tran, and C. Heuchenne. Monitoring the ratio of two normal variables using variable sampling interval exponentially weighted moving average control charts. *Quality and Reliability Engineering Interanational*, 35(1):439–460, 2019.
 - [16] H.D. Nguyen, Q.T. Nguyen, K.P. Tran, , and D.P. Ho. On the performance of vsi shewhart control chart for monitoring the coefficient of variation in the presence of measurement errors. *The International Journal of Advanced Manufacturing Technology*, pages 1–33, 2019.
 - [17] Huu-Du Nguyen and Kim Phuc Tran. Effect of the measurement errors on two one?sided shewhart control charts for monitoring the ratio of two

- normal variables. *Quality and Reliability Engineering International*, 05 2020. doi: 10.1002/qre.2656.
- [18] T. H. Nguyen, H. D. Nguyen, K. D. Tran, T. H. Truong, K. H. Phung, L. H. Nguyen, T. T. N. Le, and K. P. Tran. One-sided synthetic-rz control charts: a new method for anomaly detection. In *2019 6th NAFOS-TED Conference on Information and Computer Science (NICS)*, pages 262–267, 2019.
- [19] T. Pham-Gia, N. Turkkan, and E. Marchand. Density of the ratio of two normal random variables and applications. *Communications in Statistics - Theory and Methods*, 35(9):1569–1591, 2006.
- [20] W.A. Shewhart. *Economic Control of Quality of Manufactured Product*. Van Nostrand, New York, 1931.
- [21] Kim Phuc Tran, HD Nguyen, Quoc Thong Nguyen, and W Chaitinawat. One-sided synthetic control charts for monitoring the coefficient of variation with measurement errors. In *2018 IEEE international conference on industrial engineering and engineering management (IEEM)*, pages 1667–1671. IEEE, 2018.
- [22] K.P. Tran. Run rules median control charts for monitoring process mean in manufacturing. *Quality and Reliability Engineering International*, 2017.
- [23] K.P. Tran and S. Knoth. Steady-state arl analysis of arl-unbiased ewma-rz control chart monitoring the ratio of two normal variables. *Qual Reliab Eng Int.*, pages 1–14, 2018.
- [24] K.P. Tran, P. Castagliola, and G. Celano. Monitoring the Ratio of Two Normal Variables Using EWMA Type Control Charts. *Quality and Reliability Engineering International*, 32(2):1853–1869, 2016.
- [25] K.P. Tran, P. Castagliola, and G. Celano. Monitoring the Ratio of Population Means of a Bivariate Normal distribution using CUSUM Type Control Charts. *Statistical Papers*, 2016. In press, DOI: 10.1007/s00362-016-0769-4.
- [26] K.P. Tran, P. Castagliola, and G. Celano. Monitoring the Ratio of Two Normal Variables Using Run Rules Type Control Charts. *International Journal of Production Research*, 54(6):1670–1688, 2016.
- [27] K.P. Tran, P. Castagliola, and G. Celano. The performance of the Shewhart-RZ control chart in the presence of measurement error. *International Journal of Production Research*, 54:7504–7522, 2016.

- [28] K.P. Tran, P. Castagliola, and N. Balakrishnan. On the performance of shewhart median chart in the presence of measurement errors. *Quality and Reliability Engineering International*, 33(5):1019–1029, 2017.
- [29] K.P. Tran, C. Heuchenne, N. Balakrishnan, and M. Khoo. On the performance of coefficient of variation charts in the presence of measurement errors. *Quality and Reliability Engineering International*, In press, 2018. doi: 10.1002/qre2402.
- [30] P.H. Tran and K. P. Tran. The efficiency of CUSUM schemes for monitoring the coefficient of variation. *Applied Stochastic Models in Business and Industry*, 32(6):870–881, 2016.
- [31] Phuong Hanh Tran, Kim Phuc Tran, and Athanasios Rakitzis. A synthetic median control chart for monitoring the process mean with measurement errors. *Quality and Reliability Engineering International*, 35(4):1100–1116, 2019.
- [32] Z. Wu and T.A. Spedding. A Synthetic Control Chart for Detecting Small Shifts in the Process Mean. *Journal of Quality Technology*, 32(1):32–38, 2000.
- [33] W.C. Yeong, M.B.C. Khoo, S.L. Lim, and W.L. Teoh. The coefficient of variation chart with measurement error. *Quality Technology & Quantitative Management*, pages 1–25, 2017.